

Why was the March 16-17 2008 polar low so difficult to forecast?

B. J. K. Engdahl, University of Oslo
J. E. Kristjánsson, University of Oslo
T. Spengler, University of Bergen

At the end of the IPY-THORPEX Andøya field campaign 2008, a polar low developed in the Norwegian Sea at 71N and 13E, during the night from March 15-16. The polar low caught the researchers by surprise, as the conditions were favourable for polar low development, but the operational models placed the low further north-west. The predicted trajectory was also too fast southwards. This resulted in the 36h forecast predicting the polar low to lie several hundred kilometers south-west of the real polar low at 1200 UTC on March 16.

The forecasts accuracy for the March 16-17 polar low stands in clear contrast to the similar forecast of a previous polar low from March 3-4. In that case, the polar low was very well predicted, which made flight routes through the low, simple to plan days ahead. The goal of this study is to find out why the March 16-17 polar low was so poorly forecasted. The physical characteristics of the polar low have been investigated through satellite images, dropsondes and scatterometer, along with the fields from the ECMWF analysis. Simulations with the numerical weather prediction model weather research and forecasting (WRF), were carried out to investigate the forecasts sensitivity to certain parameters, such as time of initialisation, model resolution and different physics options.

From March 15, the conditions became favourable for polar low development. A research aircraft made a flight from Andøya to Svalbard and launched 14 dropsondes during the day. At that time a cloud band associated with a low-level convergence zone was already present, stretching from the coast of Troms in northern-Norway north-westward to the Fram strait. Cross sections representing the vertical profile of potential and equivalent potential temperature, relative humidity and wind speed were made based on the dropsonde data. These cross sections showed high low-level baroclinicity and high relative humidity up to 600hPa as well as conditional instability in the lower layers at the southern part of the section. An upper-level jet and lower-level reversed shear were found in the middle of the convergence zone.

From 1200 to 1900 UTC, satellite images show a huge increase of high clouds in that area, consistent with a cold air outbreak. On the night from March 15-16, the satellite images revealed some development within the cloud band of high clouds, with three characteristic waves. At 0600 UTC they were stationed at 73.5N 2.5W, 73N 6E and 72N 13E (see figure 1). During the night the south-easternmost wave, V1, develops further into a polar low, while the other two waves weakens or dissipate. Around noon on March 16, the polar low is stationed at 72N and 11E. Satellite images show a large area of high cloud particularly northeast of the comma shaped low. The polar low remains almost stationary throughout March 16, it only travels slightly westward. From midnight on March 17, the low travels fast southwards and makes landfall at the Norwegian coast around 63.5N 10E at 1200 UTC.

The surface pressure and 950-500hPa thickness lines from the ECMWF analysis clearly show a cold air outbreak from Greenland advancing southeastward, creating a baroclinic zone around the surface through. Along with the cold air outbreak, an area of high upper-level potential vorticity moves from the Greenland area and southeastward. At 0600 UTC on March 16 the 400hPa area with PVU above 4 is located above large parts of the Norwegian Sea (see figure 2). The positions of the waves have been adapted from the satellite image and marked with an X for each. The waves are stationed along the PV-

field. This could indicate a downwind energy propagation. Energy is transferred from V3 through V2 and ends up at V1. This can explain why V1 develops further into a polar low, while V2 and V3 dissipates shortly after. Another indication of downwind energy propagation can be seen in the absolute vorticity fields from the 925hPa level. Here, the maximum absolute vorticity propagates along the convergence zone and ends up around V1. The 950hPa potential temperature field show that the waves all form within a narrow tongue of relatively high temperatures, with V1 in the area with the highest temperatures.

Simulations were carried out with WRFv3.2. Input data from ECMWF, with 2 domains with 30km and 10km grid spacing, were used. For the high resolution runs, grid spacings of 9km and 3km were applied.

The main emphasis was on the sensitivity of the initial times. Simulations were started from 3 days prior to cyclogenesis (at 0000 UTC on March 16) to 1 day after. The results showed a clear gap in performance between the simulations initiated before and after 1200 UTC on March 15. Model runs starting before this tended to favor further development of the initial low at the northwestern side of the trough. These runs also produced a larger area of low-level high temperatures, instead of a narrow tongue of high temperatures. The upper-level PV-fields showed that the area of high PV is further away from the low, and the PV-gradient is less pronounced.

Simulations initiated at 1200 UTC on March 15 or after predicted that the initial surface low would dissipate after a short while, making the surface trough and the area with high temperatures more narrow. These runs also placed the development of the polar low closer to the real polar low. Looking at the upper-level PV in these cases show that the area of high PV air is generally closer to the low, and the PV gradient is higher. One possibility is that this strong PV-gradient contributes to the development of the polar low in the southeastern part of the trough.

The high resolution simulations were initiated at 0000 UTC on March 15 and 0000 UTC on March 16. Results from these showed much of the same features from the low resolution runs, with a much more narrow trough in the latter simulation. Fields of upper-level PV and low-level potential temperature were also similar to the low resolution runs. Hence, the higher resolution did not appear to improve the results.

A few runs were made with different physics options, all initiated at 0000 UTC on March 15. Using different parametrisation schemes for microphysics, cumulus convection and planetary boundary layer parametrisation, did not change the results of the simulations considerably.

When in-cloud latent heat contribution was switched off, the initial surface low dissipated quickly and no other lows developed. The in-cloud latent heat appears to be important both for cyclogenesis and maintenance of the polar low. In the last run, surface fluxes of sensible and latent heat were switched off. This also resulted in a quick dissipation of the initial low and no development of further lows, but as the pressure and temperature gradients were not reduced by the surface fluxes, the wind speed rose to extreme values. However, since the boundary layer parametrisation had to be switched off in this run, it can not be concluded that the surface fluxes alone contributed to this.

This study showed that the polar low development involved multiple vortices aligned along a low-level absolute vorticity streak. A possible explanation of why only one of the vortices developed into a polar low could be energy propagation along the upper-level PV-gradient. Results from the simulations systematically showed considerable better performance from the simulations initiated at 1200 UTC on March 15 and after. This could be due to the extra data provided by the dropsondes launched in the morning hours of March 15. Higher resolution did not improve the forecast, and in-cloud latent heating is crucial to both development and maintenance of the low.

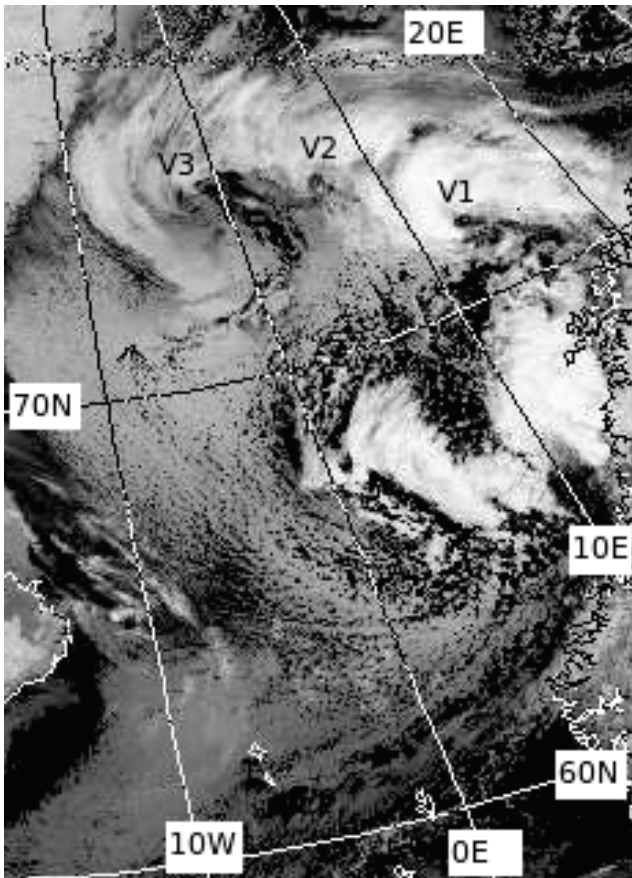


Figure 1: NOAA IR-satellite image from 0608 UTC March 16. The waves are marked V1, V2 and V3.

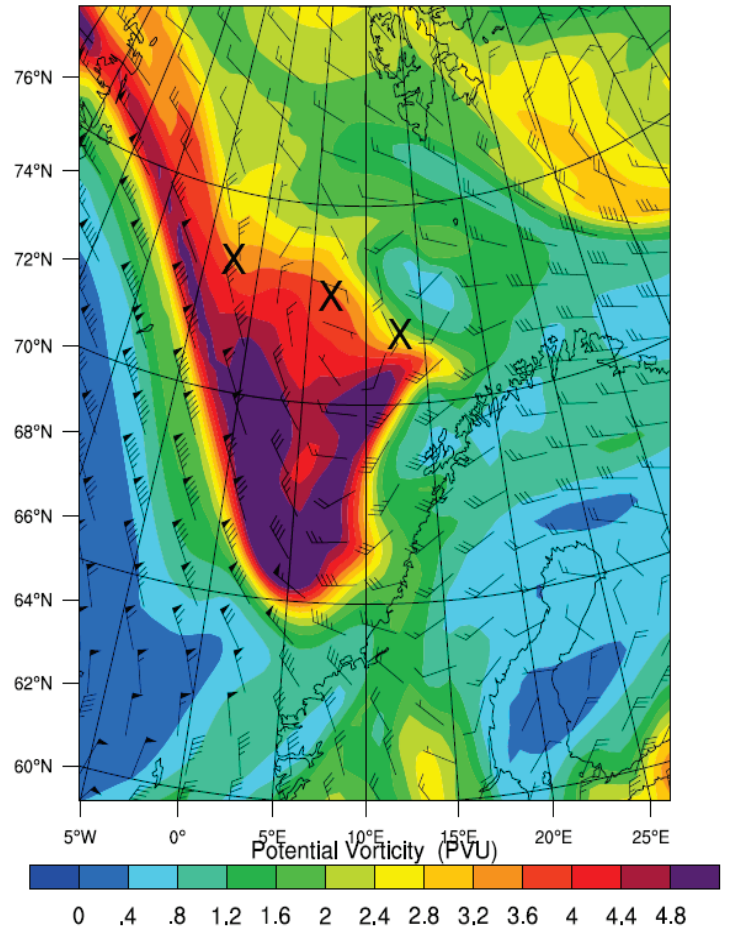


Figure 2: PV and Wind at 400hPa from the ECMWF-analysis at 0600 UTC on March 16. The position of the waves are marked with X.